

Technical Note

Superior Capsule Reconstruction Using Acellular Dermal Allograft Secured at 45° of Glenohumeral Abduction Improves the Superior Stability of the Glenohumeral Joint in Irreparable Massive Posterosuperior Rotator Cuff Tears

Burak Altintas, M.D., Hunter W. Storaci, M.S., Lucca Lacheta, M.D., Grant J. Dornan, M.Sc., Joseph J. Krob, M.D., Zachary S. Aman, B.A., Nicole Anderson, B.A., Samuel I. Rosenberg, B.A., and Peter J. Millett, M.D., M.Sc.

Purpose: The purpose of the current study was to create a dynamic cadaveric shoulder model to determine the effect of graft fixation angle on shoulder biomechanics following SCR and to assess which commonly used fixation angle (30° vs 45° of abduction) results in superior glenohumeral biomechanics. **Methods:** Twelve fresh-frozen cadaveric shoulders were evaluated using a dynamic shoulder testing system. Humeral head translation, subacromial and glenohumeral contact pressures were compared among 4 conditions: 1) Intact, 2) Irreparable supra- and infraspinatus tendon tear, 3) SCR using acellular dermal allograft (ADA) fixation at 30° of abduction, and 4) SCR with ADA fixation at 45° of abduction. **Results:** SCR at both 30° (0.287 mm, CI: -0.480 - 1.05 mm; $P < .0001$) and 45° (0.528 mm, CI: -0.239-1.305 mm; $P = .0006$) significantly decreased superior translation compared to the irreparably torn state. No significant changes in subacromial peak contact pressure were observed between any states. The average glenohumeral contact pressure increased significantly following creation of an irreparable RCT (373 kPa, CI: 304-443 vs 283 kPa, CI 214-352; $P = .0147$). The SCR performed at 45° (295 kPa, CI: 226-365, $P = .0394$) of abduction significantly decreased the average glenohumeral contact pressure compared to the RCT state. There was no statistically significant difference between the average glenohumeral contact pressure of the intact state and SCR at 30° and 45°. **Conclusion:** SCR improved the superior stability of the glenohumeral joint when the graft was secured at 30° or 45° of glenohumeral abduction. Fixation at 45° of glenohumeral abduction provided more stability than did fixation at 30°. **Clinical Relevance:** Grafts attached at 45° of glenohumeral abduction biomechanically restore the glenohumeral stability after SCR using ADA better than fixation at 30° of glenohumeral abduction.

Steadman Philippon Research Institute, Vail, Colorado, U.S.A. (B.A., H.W.S., L.L., G.J.D., J.J.K., Z.S.A., N.A., S.I.R., P.J.M.); The CORE Institute, Phoenix, Arizona, U.S.A. and University of Arizona College of Medicine Phoenix, Phoenix, Arizona, U.S.A. (B.A.); Center for Musculoskeletal Surgery, Charité Universitätsmedizin Berlin, Berlin, Germany (L.L.); Sidney Kimmel Medical College at Thomas Jefferson University, Philadelphia, Pennsylvania, U.S.A. (Z.S.A.); and The Steadman Clinic, Vail, Colorado, U.S.A. (P.J.M.)

The authors report the following potential conflicts of interest or sources of funding: P.J.M. reports grants, personal fees and other from Arthrex Inc, personal fees from Springer Publishing, personal fees from Medbridge, stock options from VuMedi, part owner of ProofPoint Biologics, research support from Steadman Philippon Research Institute, institutional funding from Smith & Nephew, Siemens, and Össur, outside the submitted work. B.A. reports other from Steadman Philippon Research Institute and fellowship support from Arthrex, Inc, outside the submitted work. H.W.S. reports employment from Steadman Philippon Research Institute, outside the submitted work. L.L. reports employment from Steadman Philippon Research

Institute, outside the submitted work. G.J.D. reports employment from Steadman Philippon Research Institute, outside the submitted work. J.J.K. reports employment from Steadman Philippon Research Institute, outside the submitted work. Z.S.A. reports other from Steadman Philippon Research Institute, outside the submitted work. N.A. reports employment from Steadman Philippon Research Institute, outside the submitted work. S.I.R. reports employment from Steadman Philippon Research Institute, outside the submitted work. Full ICMJE author disclosure forms are available for this article online, as [supplementary material](#).

Received December 3, 2021; accepted October 20, 2022.

Address correspondence to Peter J. Millett, M.D., M.Sc., Steadman Philippon Research Institute, The Steadman Clinic, 181 West Meadow Drive, Suite 400, Vail, Colorado 81657, U.S.A.. E-mail: drmillett@thesteadmanclinic.com

© 2022 by the Arthroscopy Association of North America

0749-8063/211718/\$36.00

<https://doi.org/10.1016/j.arthro.2022.10.037>

Introduction

In an aging and increasingly active population, irreparable rotator cuff tears (RCTs) present a particularly complex and difficult challenge. The prevalence of full-thickness RCTs in the general population is approximately 22% and increases with patient age.^{1,2} The reported prevalence of massive RCTs has been as high as 40% of all RCTs.^{3,4} Tissue inelasticity, poor tendon quality, adhesions, muscle atrophy, and fatty infiltration can all contribute to irreparability. Some treatment options exist for these tears, including partial repair,⁵ patch-augmented repair,⁶ bridging rotator cuff reconstruction with a graft,⁷ latissimus dorsi tendon transfer,⁸ and arthroscopic superior capsule reconstruction (SCR).⁹

Arthroscopic SCR was first reported by Mihata et al.¹⁰ in a 2012 cadaveric biomechanical study as an effective method for reducing superior humeral head translation. It is a minimally invasive surgical technique for the treatment of irreparable superior RCTs. In this operation, a graft is attached medially to the superior glenoid and laterally to the greater tuberosity to reconstruct the superior shoulder capsule. While Mihata et al. performed biomechanical studies on the effects of different graft thickness,¹¹ capsular continuity,¹² and acromioplasty¹³ in SCRs with a tensor fasciae latae (TFL) graft, there is limited number of published biomechanical studies on SCR using acellular dermal allograft (ADA).¹⁴ Moreover, there is no consensus regarding the graft fixation angle to enhance glenohumeral stability without sacrificing range of motion or risking graft tear.¹⁵

Despite the significant improvement in clinical outcome scores following SCR, the high rate of graft tears with ADA remains concerning and raises questions regarding the adequate graft fixation angle due to the importance of maintaining appropriate graft tension at 90° of shoulder abduction and preventing graft tears at 0° of shoulder abduction. The appropriate graft tension and optimal abduction angle during graft fixation remain to be determined. A previous biomechanical study by Mihata et al. used a shoulder model with loading of the muscles surrounding the glenohumeral joint and showed that SCR using an ADA partially reduced superior translation and completely restored subacromial contact and superior glenohumeral joint force.¹⁴ Another study by the same group did not show a difference between graft fixation at 10° and 30° of glenohumeral abduction.¹¹ However, the most common fixation angles for SCR involve higher degrees of glenohumeral abduction and the reported shoulder model prohibits the dynamic movement of the humeral head with deltoid contraction. Thus, previous studies using this model are limited in replicating the kinematics of the shoulder. The purpose of the current study

was to create a dynamic cadaveric shoulder model to determine the effect of graft fixation angle on shoulder biomechanics following SCR and to assess which commonly used fixation angle (30° vs 45° of abduction) results in superior glenohumeral biomechanics. It was hypothesized that SCR would reduce humeral head superior translation, glenohumeral contact pressure and subacromial contact pressure of the native state. Additionally, graft fixation at 45° of abduction would show increased glenohumeral stability compared to fixation at 30° of abduction.

Methods

Research was performed at the Steadman Philippon Research Institute, Vail, Colorado.

Specimen Preparation

Twelve fresh-frozen male cadaveric shoulder specimens (mean age, 56.3 years; range, 51-64 years) with no evidence of osteoarthritis, osteoporosis, prior injury or surgery to the shoulder were used for this study. Institutional review board approval was not required because deidentified cadaveric specimens are exempt from review at our institution. The cadaveric specimens used in this study were donated to a tissue bank for the purpose of medical research and then purchased by our institution. All specimens were stored at -20° C and thawed at room temperature for 24 hours before preparation. The specimens were assessed by two orthopedic surgeons (B.A. and L.L.). Each specimen underwent a diagnostic arthroscopy before testing to confirm the absence of intraarticular pathology and was excluded if any evidence of labral or rotator cuff pathologies existed. Sharp dissection to bone was then performed. All soft tissues were removed except for the teres minor, infraspinatus, supraspinatus, and subscapularis muscle bodies and their respective insertions. All ligamentous structures and capsular attachments surrounding the glenohumeral joint were preserved as well. During specimen preparation for each shoulder, range of motion (abduction-adduction and internal-external rotation) was actively tested to detect and reduce the potential effect of joint stiffness and rigidity. The inferior portion of the scapula was potted in a rectangular mold filled with PMMA (polymethyl methacrylate, Fricke Dental International Inc., Streamwood, IL), preserving the axial orientation by positioning the scapular spine parallel to the base. The humeral shaft was transected 6 cm distal to the deltoid tuberosity and fixed in a half cylindrical mold filled with PMMA to allow controlled abduction during testing (Fig 1, A and B).

Testing Setup

The rectangular scapular potting was affixed to a custom jig in neutral position, as determined by setting

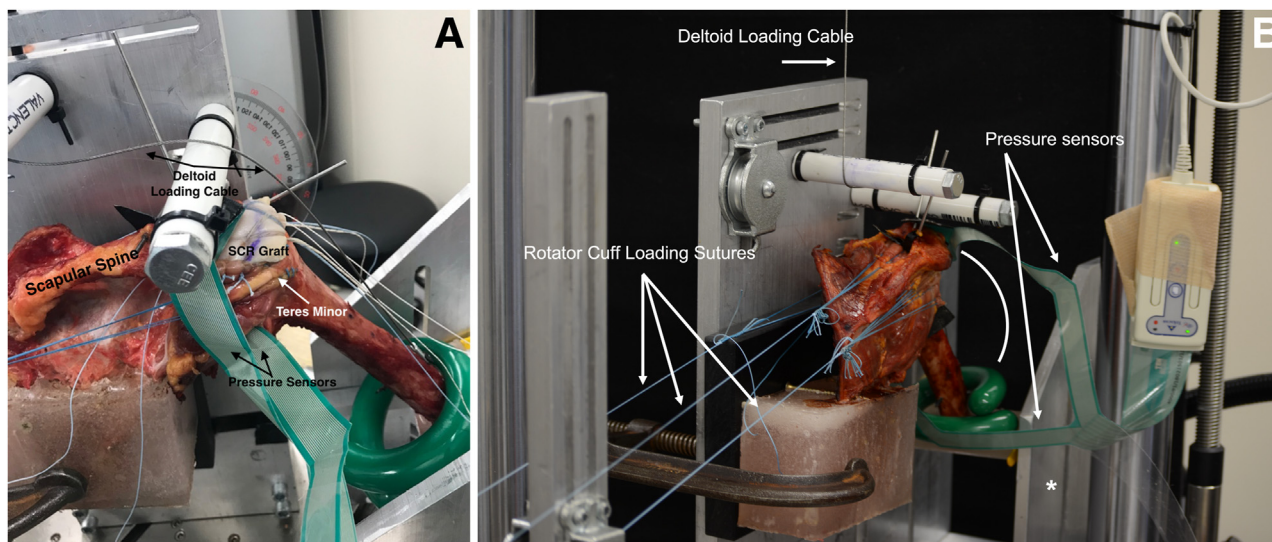


Fig 1. (A and B) Posterior view of the shoulder testing system for a right shoulder. *Customized fixture to allow abduction (curved line).

the spine of the scapula parallel to the plane of the actuator of the dynamic tensile testing machine (Instron ElectroPuls E10000, Instron Corp., Norwood, MA). Following fixation, physiological rotator cuff muscle forces were simulated by loading the intact musculature with free weights suspended by a pulley system. Each rotator cuff tendon was sutured using high-strength sutures (#2 FiberWire, Arthrex, Inc., Naples, FL) in a Krackow locked running stitch fashion and subsequently connected to the free weights. The rotator cuff loading protocol for each testing position based on data of the cross-sectional area of each muscle were based of the study by Keating et al.¹⁶ and were as follows: 6.7 N, supraspinatus; 15.6 N, infraspinatus and teres minor; and 24.5 N, subscapularis. A wood screw was inserted in the deltoid tuberosity and tied to a steel cable connected to the actuator. A pulley system was used to approximate the anatomical pull of the deltoid muscle. An 8.9-N force was used on the distal aspect of the humerus to approximate the weight of the arm. The potted humerus was positioned in a customized fixture after loading to allow for free abduction during testing, while restricting flexion and rotation. Two rigid wood struts were glued to the faces of the hemi-cylindrical potting of the humerus and lubricated to minimize contact friction during abduction. Prior to the final testing for this study, this physiological loading protocol was validated by true anteroposterior and axillary radiographs of the glenohumeral joint to assure proper seating of the humeral head on the glenoid. This was established by the continuity of the scapulohumeral arch formed by the medial proximal humerus and lateral border of the scapula, as well as the concentric relationship between the humeral head and the glenoid

cavity. The radiographs and positioning were reviewed by two orthopedic surgeons (B.A. and L.L.).

After complete fixation of the specimen to the dynamic tensile testing machine, a two-pronged pressure sensor (Pressure Mapping Sensor 4000 for I-Scan, Tekscan, Inc., Boston, MA) was carefully fixed on the surface of the glenoid fossa through an incision of the inferior capsule and an additional incision in the rotator interval, while avoiding the violation of the anterior or posterior capsule. The second prong of the sensor was then positioned on the undersurface of the acromion in an optimal position determined by previous pilot testing. Briefly, the position of the sensor was kept consistent throughout testing by securing the sensors to the glenoid and acromion using screws and localizing the baseline pressure observed from the sensors to the same area on the pressure map (Fig 2). All specimens were kept moist with 0.9% saline throughout experimentation.

Surgical Technique

Two orthopedic surgeons (B.A. and L.L.) performed the procedure. An open SCR using an ADA (40 mm × 70 mm × 3.0 mm ArthroFLEX, Arthrex Inc., Naples, FL) was performed in all specimens, as previously described.¹⁷ Briefly, the supraspinatus and infraspinatus muscles and tendons were removed completely. The long head of the biceps was detached at its insertion to the superior labrum and was removed from the bicipital sheath. Anterior-posterior widths and medial-lateral dimensions of the ADA were matched to the superior glenoid, as well as to the rotator cuff footprint area, as described by Mihata's biomechanical studies.¹⁰ Next, three 3 mm × 12.4 mm PEEK suture

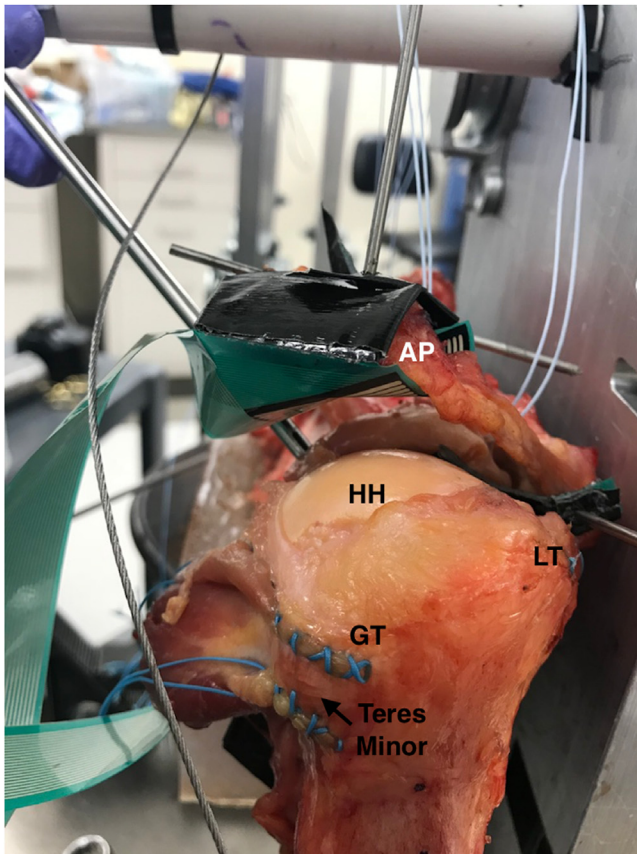


Fig 2. Lateral view photograph depicting the massive tear state in a right shoulder secured to the testing system. AP, acromion process; GT, greater tuberosity; HH, humeral head; LT, lesser tuberosity.

anchors (SutureTak, Arthrex Inc.) loaded with high strength suture, (#2 FiberWire, Arthrex Inc.) were inserted into the superior glenoid. The sutures were passed through the graft in a horizontal mattress fashion and tied over it securely. The humeral sided fixation was performed in a double-row transosseous equivalent fashion using 4 biocomposite 4.75 mm × 19.1 mm knotless suture anchors (SwiveLock, Arthrex Inc.) loaded with ultra-high-strength suture tape loops (FiberTape, Arthrex Inc.). Following the first fixation at 30° or 45° of abduction and subsequent testing, the lateral row anchors were removed, and the graft was retensioned for the second fixation at the respective angle of abduction before the lateral row anchors were reinserted (Fig 3). The fixation angle order was randomized between shoulders. Additional sutures were passed through the lateral portion of the graft and were connected to a dynamometer (SF-500 Force Gauge, Yueqing Aliyiqi Instruments Co., Ltd, Zhejiang, China) to fix the graft using the same tension for all specimens. The same tension was applied to the graft during lateral fixation in both abduction angles to minimize variability as the graft can be tightened differently. While

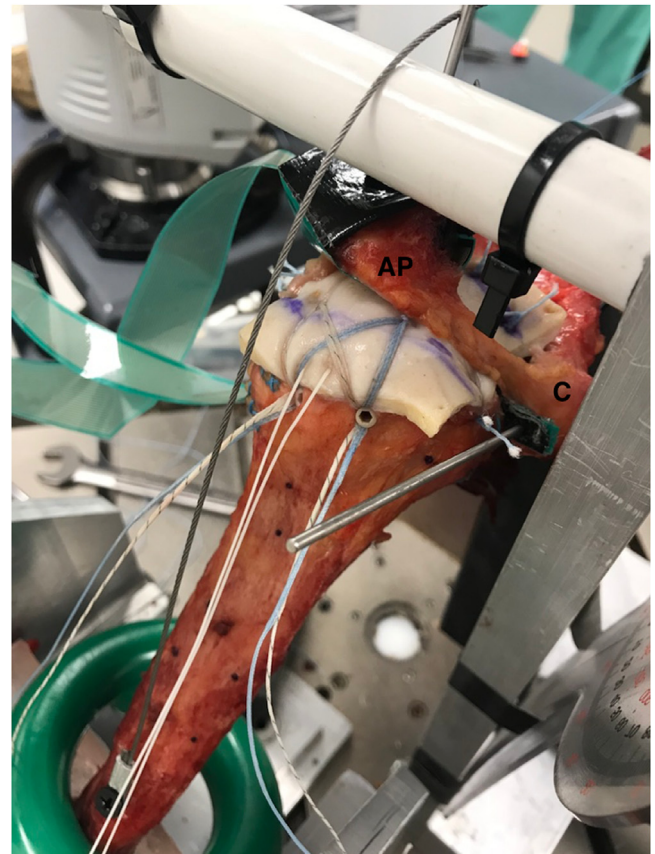


Fig 3. Superior capsule reconstruction in a right shoulder. AP, acromion process; C, coracoid.

the graft tension changes during abduction, this method was used to limit the variation of initial graft tensioning prior to testing. The reconstruction was completed by suturing the allograft to the subscapularis and infraspinatus tendons in a side-to-side fashion using high-strength suture (#2 FiberWire, Arthrex Inc.). Complete SCR is shown in Fig 3.

Biomechanical Testing

Each specimen was subjected to dynamic biomechanical testing employing a dynamic tensile testing machine to simulate an abduction force on the humerus and allow for controlled dynamic motion analysis. The biomechanical testing occurred in three sequential phases: 1. Calibration 2. Dynamic motion 3. Positional testing. For calibration, the hydraulic actuator was moved to its minimum position, and the deltoid insertion cable was tensioned to the point just before abduction of the humerus occurred, defining neutral position for this testing state. From this position, the tensile testing machine applied a force to the deltoid insertion to abduct the humerus in 10° increments. The digital position of the actuator was recorded at each angle. This enabled determination of the relationship between actuator position and abduction angle for each

Table 1. Intact-subtracted Superior Translation by State

	State	EM Mean (mm)	95% CI	
Group Averages	Massive RCT	1.59	0.82 - 2.35	
	SCR at 30°	0.29	-0.48 - 1.05	
	SCR at 45°	0.53	-0.24 - 1.31	
	Comparison	Mean Difference (mm)	95% CI	P Value
Pairwise Comparisons	Massive RCT vs SCR at 30°	1.30	0.68 - 1.91	<.0001
	Massive RCT vs SCR at 45°	1.06	0.44 - 1.67	.0006
	SCR at 30° vs SCR at 45°	-0.24	-0.86 - 0.37	.3923

Group averages and pairwise between-state comparisons. Results are derived from 2-factor linear mixed-effects models with tested abduction angle assumed constant.

EM Mean, estimated marginal mean; 95% CI, Holm-adjusted 95% confidence intervals.

testing state, allowing for calculation of the abduction angle based on actuator position. Subacromial and glenohumeral contact pressures were recorded using the pressure sensors.

The dynamic motion was analyzed following calibration. For this, the actuator of the tensile testing machine was returned to starting position, returning the humerus to neutral position, and then moved to abduct the shoulder throughout its entire range of motion, while at the same time recording pressure data. For positional testing, the actuator was used to abduct the humerus to 30° and 60° with neutral rotation and a custom fixture secured the humerus at that angle. A coordinate measuring machine (ROMER Absolute Arm, Hexagon Manufacturing Intelligence, Cobham, Surrey, Great Britain) was then utilized to record the position of 7 fiducial points at neutral position (minimally abducted) as well as for 30°, and 60° of abduction. The 3-dimensional translation of the humeral head was calculated by recording the humeral head center of rotation at each angle and comparing it to the humeral head center of rotation in the intact state. To achieve this, the coordinate measuring machine was used to record the positions of 4 points on the scapula prior to potting the scapula in PMMA and to develop the joint coordinate frame (J.C.F.) for the scapula as previously published by Wu et al.¹⁸ All fiducial markers taken with the coordinate measuring machine during testing were transformed into the scapular JCF to allow for reporting of translations in the terms of each specimen's scapular frame. The fiducial markers on the humerus were recorded in a similar fashion. After completed testing, the humerus was disarticulated and the fiducial markers on the humerus, along with a cloud of points on the humeral head, were recorded. These were used to calculate the humeral head center of rotation as previously published by Meskers et al.¹⁹ All calculations were done using custom software Python 3.4.

Statistical Analysis

All measurements were performed thrice, and the mean value was used for data analyses. To match the repeated measures experimental design, random-intercepts linear mixed-effects models were used to compare translation measurements (superior, anterior, and lateral) and pressure measurements (glenohumeral and subacromial; peak pressure, contact area, and average pressure) among shoulder states. Estimated marginal means were used to make all pairwise-comparisons and the Holm-Bonferroni method was used to control the familywise error rate to 5% among this set of comparisons. Residual diagnostics were inspected to ensure model fit and that assumptions were met. The statistical software R version 3.5.0 was used for all plots and analyses (access date March 16, 2019; R Core Team, Vienna Austria; with additional packages nlme, emmeans, and ggplot2).²⁰ The sample size was determined based on feasibility and was comparable to other similar studies in the literature. As a simplification of the full mixed-effect modeling analysis, statistical power was considered with regard to the repeated-measures pairwise comparisons between experimental states. Assuming an alpha level of 0.05, two-tailed testing, and parametric dependent groups comparisons of means, 12 specimens are sufficient to detect an effect size of Cohen's $d = 0.89$ with 80% statistical power. Thus, between-state differences more subtle than $d = 0.89$ cannot be ruled out by this study.

Results

Effect of SCR on Superior Translation

Creation of an irreparable massive RCT increased superior translation averaged over the levels of different abduction angles (1.59 mm, CI: 0.82 – 2.35 mm). After SCR using the ADA performed at either 30° or 45° of abduction, the superior translation decreased significantly compared to that in the irreparably torn state (Table 1). The superior translation was measured

Table 2. Subacromial Peak Pressure Results by State

	State	EM Mean (kPa)	95% CI	
Group Averages	Intact	430	191 - 670	
	Massive RCT	580	341 - 819	
	SCR at 30°	546	307 - 786	
	SCR at 45°	584	344 - 823	
	Comparison	Mean Difference (kPa)	95% CI	P Value
Pairwise Comparisons	Intact vs Massive RCT	-150	-400 - 101	>.999
	Intact vs SCR at 30°	-116	-366 - 135	>.999
	Intact vs SCR at 45°	-153	-404 - 97	>.999
	Massive RCT vs SCR at 30°	34	-217 - 284	>.999
	Massive RCT vs SCR at 45°	-4	-254 - 247	>.999
	SCR at 30° vs SCR at 45°	-38	-288 - 213	>.999

Group averages and pairwise between-state comparisons.

EM Mean, estimated marginal mean; 95% CI, Holm-adjusted 95% confidence intervals.

as 0.29 mm (CI: -0.48 -1.05 mm) at 30° of abduction ($P < .0001$) and as 0.53 mm (CI: -0.24 - 1.31 mm) at 45° of abduction ($P = .0006$). There were no differences between the decrease of superior translation between fixation at 30° or 45° of abduction ($P = .3923$).

Effect of SCR on Anterior and Lateral Translation

Creation of an irreparable massive RCT did not significantly affect the anterior translation averaged over the levels of different abduction angles (-0.28 mm, CI: -1.22- 0.66 mm). After SCR using the ADA performed at either 30° (0.58 mm, CI: -0.36-1.52 mm; $P = .1784$) or 45° (0.53 mm, CI: -0.41-1.46 mm; $P = .1784$) of abduction the anterior translation showed no significant changes compared with that in the irreparably torn state. No significant differences were observed between fixation at 30° or 45° of abduction ($P = .9033$).

Similar results were found for changes in lateral translation. Creation of an irreparable massive RCT did

not significantly affect the lateral translation averaged over the levels of different abduction angles (-0.15 mm, CI: -0.29 - 0.59 mm). After SCR using the ADA performed at either 30° (-0.21 mm, CI: -0.66-0.23 mm; $P = .1291$) or 45° (-0.0153 mm, CI: -0.46-0.43 mm; $P = .5384$) of abduction the anterior translation showed no significant changes compared with that in the irreparably torn state. No significant differences were observed between fixation at 30° or 45° of abduction ($P = .5384$).

Effect of SCR on Subacromial Contact Pressure

The peak subacromial contact pressure increased following creation of an irreparable RCT (580 kPa, CI: 341- 819 kPa) compared to intact state (430 kPa, CI: 191- 670 kPa), but this did not reach statistical significance ($P = 1$, Table 2). After SCR performed at either 30° (546 kPa, CI: 307-786 kPa) or 45° of abduction (584 kPa, CI: 344-823 kPa), the subacromial peak contact pressure did not change significantly compared to the

Table 3. Glenohumeral Peak Pressure Results by State

	State	EM Mean (kPa)	95% CI	
Group Averages	Intact	547	394 - 699	
	Massive RCT	814	661 - 967	
	SCR at 30°	760	607 - 913	
	SCR at 45°	718	565 - 871	
	Comparison	Mean Difference (kPa)	95% CI	P Value
Pairwise Comparisons	Intact vs Massive RCT	-68	-246 - 110	.014
	Intact vs SCR at 30°	-213	-391 - 35	.063
	Intact vs SCR at 45°	-172	-350 - 6	.164
	Massive RCT vs SCR at 30°	54	-124 - 232	>.999
	Massive RCT vs SCR at 45°	96	-82 - 274	.731
	SCR at 30° vs SCR at 45°	42	-136 - 220	>.999

Group averages and pairwise between-state comparisons.

EM Mean, estimated marginal mean; 95% CI, Holm-adjusted 95% confidence intervals.

intact state ($P = 1$). Similar results were achieved for average subacromial contact pressures.

Effect of SCR on Glenohumeral Contact Pressure

The glenohumeral peak contact pressure increased significantly following creation of an irreparable RCT (814 kPa, CI: 661-967 kPa) compared to intact state (547 kPa, CI: 394-699 kPa; Table 3). While the SCR performed at either 30° (760 kPa, CI: 607-913 kPa) or 45° (718 kPa, CI: 565-871 kPa) of abduction decreased the glenohumeral peak contact pressure, this difference did not reach statistical significance. No statistical significance was found between glenohumeral peak contact pressures between the intact and SCR states at 30° ($P = .0625$) or 45° of abduction ($P = .1644$). The results were similar for the comparison between the glenohumeral peak contact pressure following irreparable RCT and SCR states at 30° ($P = 1$) or 45° of abduction ($P = .7307$). No significant differences were observed between fixation at 30° or 45° of abduction ($P = 1$).

The average glenohumeral contact pressure increased significantly following creation of an irreparable RCT (373 kPa, CI: 304-443 kPa vs 283 kPa, CI 214-352 kPa; $P = .0147$). The SCR performed at either 30° (301 kPa, CI: 232-370 kPa) or 45° (295 kPa, CI: 226-365 kPa) of abduction decreased the average glenohumeral contact pressure compared to the RCT state. This difference reached statistical significance following SCR at 45° of abduction ($P = .0394$) but did not reach statistical significance after SCR fixation at 30° ($P = .0526$). No significant differences were observed between fixation at 30° or 45° of abduction ($P = 1$). Moreover, there were no statistically significant differences between the average glenohumeral contact pressure between the intact state and SCR at 30° and 45° of abduction ($P = 1$ for each comparison).

Discussion

The main finding of the current study is that SCR decreased the superior translation of the humeral head following irreparable posterolateral RCT and that the fixation at 45° of glenohumeral abduction provided better restoration of glenohumeral contact pressure than did the fixation at 30°. In a previous study, the biomechanical evaluation of the SCR using a TFL graft for a single tendon supraspinatus tear demonstrated improved stability and reduction of subacromial impingement compared to patch grafting of the supraspinatus tendon.¹⁰ Moreover, greater reductions of subacromial peak contact pressure were observed with SCR using an 8-mm TFL graft compared to 4 mm thick grafts, indicating improved stability of the joint.¹¹ Further biomechanical studies conducted by Mihata et al. provided further evidence in SCR's benefit in reducing subacromial joint impingement and improving overall joint stability in cases of irreparable

supraspinatus tears.¹¹⁻¹⁴ However, SCR is used more frequently for the treatment of massive irreparable RCTs rather than tears of the supraspinatus alone. Thus, the current study analyzed the effect of SCR on restoring the glenohumeral stability for an irreparable tear that involved both the supraspinatus and infraspinatus tendons.

Recent biomechanical studies focused on the effect of SCR using alternative grafts including ADA¹⁴ and the long head of the biceps (LHB)²¹. Mihata et al. compared the biomechanics of SCR using TFL with ADA and concluded beneficial effects for both grafts in restoring glenohumeral stability.¹⁴ While SCR using the TFL completely restored the superior translation, superior glenohumeral joint force and subacromial contact pressure, SCR with ADA showed a similar effect except for the partial restoration of the superior translation.¹⁴ They observed lengthening of the ADA after testing, while the TFL graft length remained unchanged.¹⁴ This may predispose the SCR with ADA for earlier failure. However, the early clinical outcomes have been promising.¹⁵ El-shaar et al. analyzed SCR with an LHB autograft in a cadaveric massive rotator cuff tear model and showed it to be biomechanically equivalent to SCR with a TFL autograft in the prevention of superior humeral migration.²¹ In comparison of stress required to superiorly translate a humerus for 1.5 cm, LHB autografts required significantly more stress for superior translation compared to TFL autografts.²¹ The results of the present study are in line with the previously published literature showing a positive biomechanical effect of SCR on glenohumeral stability in the coronal plane.

The optimal tensioning angle for SCR remains unclear. Mihata et al. reported that fixation of the TFL graft with a glenohumeral abduction of 10° versus 30° at time of reconstruction showed similar results in restoring the stability, specifically in reduction of superior translation and peak subacromial pressure.¹¹ Though not statistically significant, trends toward less superior translation were observed with graft placement at 30° glenohumeral abduction compared to 10° abduction.¹¹ Further investigation was conducted by Hast et al., who used a paradigm coupling in vitro, in vivo and in silico modeling techniques to assess SCR graft strains after fixation in different angles.²² They showed that motions involving posterior shoulder rotation, such as back washing, lead to graft strains that may cause failure.²² Moreover, the ideal placement to counteract strain without excessive graft slack was determined to be a humeral orientation of 25° abduction and 20° internal rotation.²² This is very important as the graft fixation angles in the reported clinical outcome studies vary widely between neutral abduction²³ to 70° of elevation and 10° of abduction.²⁴ The present study showed that graft fixation at 45° of abduction provided better improvement of glenohumeral contact pressure

compared to fixation at 30° of abduction. Determining the optimal graft fixation angle is crucial in getting the most consistent improvement in shoulder function without early graft failure after SCR.

Limitations

There were some limitations to the current study. Inherent to a time 0 cadaveric study, the results did not reflect the biological incorporation of the dermal allograft and its effects on reconstruction performance. Also, the effects of various tension angles on long-term stability is not known, and it is possible that while fixation at 45° better improved glenohumeral contact pressure, fixation at lower abduction angles might result in better clinical function or graft incorporation. The physiological shoulder motion involves combination of scapular motion, flexion, rotation, and abduction. Controlling abduction while fixing the other elements may limit the clinical translation of the results. However, it provides dynamic assessment while controlling other parameters. The opening in the inferior capsule, which was created to insert the glenohumeral contact sensor, could have contributed to less superior humeral head migration. Furthermore, the multiple testing conditions may have produced certain laxity in the surrounding soft tissue structures including the ADA. However, this effect was limited by randomizing the order of the testing. In addition, the effect of dependent variables was limited by using the same materials and commercially available dermal allografts for every reconstruction. Further, multiple pilot tests were performed to establish reproducible and highly accurate testing procedures with this shoulder testing model.

Conclusion

SCR improved the superior stability of the glenohumeral joint when the graft was attached at 30° or 45° of glenohumeral abduction. The fixation at 45° of glenohumeral abduction provided more stability than did the fixation at 30°.

References

1. Yamamoto A, Takagishi K, Osawa T, et al. Prevalence and risk factors of a rotator cuff tear in the general population. *J Shoulder Elbow Surg* 2010;19:116-120.
2. Minagawa H, Yamamoto N, Abe H, et al. Prevalence of symptomatic and asymptomatic rotator cuff tears in the general population: From mass-screening in one village. *J Orthop* 2013;10:8-12.
3. Greenspoon JA, Petri M, Warth RJ, Millett PJ. Massive rotator cuff tears: Pathomechanics, current treatment options, and clinical outcomes. *J Shoulder Elbow Surg* 2015;24:1493-1505.
4. Bedi A, Dines J, Warren RF, Dines DM. Massive tears of the rotator cuff. *J Bone Jt Surg Am* 2010;92:1894-1908.
5. Kim S-J, Kim S-H, Lee S-K, Seo J-W, Chun Y-M. Arthroscopic repair of massive contracted rotator cuff tears: Aggressive release with anterior and posterior interval slides do not improve cuff healing and integrity. *J Bone Jt Surg Am* 2013;95:1482-1488.
6. Petri M, Warth RJ, Horan MP, Greenspoon JA, Millett PJ. Outcomes after open revision repair of massive rotator cuff tears with biologic patch augmentation. *Arthroscopy* 2016;32:1752-1760.
7. Gupta AK, Hug K, Boggess B, Gavigan M, Toth AP. Massive or 2-tendon rotator cuff tears in active patients with minimal glenohumeral arthritis. *Am J Sports Med* 2013;41:872-879.
8. Irlenbusch U, Bracht M, Gansen HK, Lorenz U, Thiel J. Latissimus dorsi transfer for irreparable rotator cuff tears: A longitudinal study. *J Shoulder Elbow Surg* 2008;17:527-534.
9. Mihata T, Lee TQ, Watanabe C, et al. Clinical results of arthroscopic superior capsule reconstruction for irreparable rotator cuff tears. *Arthroscopy* 2013;29:459-470.
10. Mihata T, McGarry MH, Pirolo JM, Kinoshita M, Lee TQ. Superior capsule reconstruction to restore superior stability in irreparable rotator cuff tears: A biomechanical cadaveric study. *Am J Sports Med* 2012;40:2248-2255.
11. Mihata T, McGarry MH, Kahn T, Goldberg I, Neo M, Lee TQ. Biomechanical effect of thickness and tension of fascia lata graft on glenohumeral stability for superior capsule reconstruction in irreparable supraspinatus tears. *Arthroscopy* 2016;32:418-426.
12. Mihata T, McGarry MH, Kahn T, Goldberg I, Neo M, Lee TQ. Biomechanical role of capsular continuity in superior capsule reconstruction for irreparable tears of the supraspinatus tendon. *Am J Sports Med* 2016;44:1423-1430.
13. Mihata T, McGarry MH, Kahn T, Goldberg I, Neo M, Lee TQ. Biomechanical effects of acromioplasty on superior capsule reconstruction for irreparable supraspinatus tendon tears. *Am J Sports Med* 2016;44:191-197.
14. Mihata T, Bui CNH, Akeda M, et al. A biomechanical cadaveric study comparing superior capsule reconstruction using fascia lata allograft with human dermal allograft for irreparable rotator cuff tear. *J Shoulder Elbow Surg* 2017;26:2158-2166.
15. Altintas B, Scheidt M, Kremser V, et al. Superior capsule reconstruction for irreparable massive rotator cuff tears: Does it make sense? A systematic review of early clinical evidence. *Am J Sports Med* 2020;48:3365-3375.
16. Keating JF, Waterworth P, Shaw-Dunn J, Crossan J. The relative strengths of the rotator cuff muscles. A cadaver study. *J Bone Joint Surg Br* 1993;75:137-140.
17. Altintas B, Higgins B, Anderson N, Millett PJ. Superior capsule reconstruction for the treatment of irreparable rotator cuff tears. *Oper Tech Orthop* 2018;28:226-231.
18. Wu G, Siegler S, Allard P, et al. ISB recommendation on definitions of joint coordinate system of various joints for the reporting of human joint motion—Part I: Ankle, hip, and spine. International Society of Biomechanics. *J Biomech* 2002;35:543-548.
19. Meskers CGM, van der Helm FCT, Rozendaal LA, Rozing PM. In vivo estimation of the glenohumeral joint rotation center from scapular bony landmarks by linear regression. *J Biomech* 1997;31:93-96.
20. R Development Core Team. *R: A Language and Environment for Statistical Computing*. Vienna, Austria: R Foundation for Statistical Computing, 2016.

21. El-shaar R, Soin S, Nicandri G, Maloney M, Voloshin I. Superior capsular reconstruction with a long head of the biceps tendon autograft: A cadaveric study. *Orthop J Sport Med* 2018;6:232596711878536.
22. Hast MW, Schmidt EC, Kelly JD, Baxter JR. Computational optimization of graft tension in simulated superior capsule reconstructions. *J Orthop Res* 2018;36:2789-2796.
23. Hirahara AM, Andersen WJ, Panero AJ. Superior capsular reconstruction : Clinical outcomes after minimum 2-year follow-up. *Am J Orthop* 2017;46:266-272, 278.
24. de Campos Azevedo CI, Ângelo ACLPG, Vinga S. Arthroscopic superior capsular reconstruction with a minimally invasive harvested fascia lata autograft produces good clinical results. *Orthop J Sport Med* 2018;6:232596711880824.